Journal of Physiology (2002), **538.2**, *pp.* 391–404
DOI: 10.1013/jphysiol.2001.012961

www.jphysiol.org

An inward rectifier K^+ channel at the basolateral membrane of the mouse distal convoluted tubule: similarities with Kir4–Kir5.1 heteromeric channels

Stéphane Lourdel, Marc Paulais, Françoise Cluzeaud *, Marcelle Bens *, Masayuki Tanemoto †, Yoshihisa Kurachi †, Alain Vandewalle * and Jacques Teulon

*INSERM U426 and * INSERM U478, Institut Fédératif de Recherche 02, Faculté de Médecine Xavier Bichat, Paris, France and † Department of Pharmacology II, Graduate School of Medicine, Osaka University, Yamada-oka 2-2, Suita, Osaka 565-0871, Japan*

In this study, K^+ channels present in the basolateral membrane of the distal convoluted tubule (DCT) were investigated using patch-clamp methods. In addition, Kir4.1, Kir4.2 and Kir5.1 inward rectifier channels were investigated using RT-PCR and immunohistochemistry (Kir4.1). DCTs were microdissected from collagenase-treated mouse kidneys. One type of K^+ channel was detected in about 50 % of cell-attached patches from the DCT basolateral membrane; this channel was inwardly rectifying and had an inward conductance (g_{in}) of ~40 pS at an external [K^+] of 145 mM. The current–voltage relationship was linear when inside-out patches were exposed to a Mg^{2+}-free medium. Mg^{2+} at a concentration of 1.2 mM considerably reduced the outward conductance (g_{out}), yielding a g_{in}/g_{out} ratio of ~4.7. The polycation spermine (5×10^{-7} M) reduced the open probability (P_o) by 50 %. Channel activity was dependent upon the intracellular pH, with acid pH decreasing, and basic pH increasing, P_o. Internal ATP (2 mM) and Ca^{2+} (up to 10^{-3} M) had no effect. Channel activity declined irreversibly when the inner side of the patch was exposed to Mg^{2+}. Kir4.1, Kir4.2 and Kir5.1 mRNAs were all detected in the DCT. The Kir4.1 protein co-localised with the Na^+–Cl^- cotransporter, which is specific to the DCT, and was located on basolateral membranes. The DCT K^+ channel differs from other functionally identified renal K^+ channels with regard to its inhibition by spermine and insensitivity to internal ATP and Ca^{2+}. At the current state of knowledge, the channel is similar to Kir4.1–Kir5.1 and Kir4.2–Kir5.1 heteromeric channels, but not to Kir4.1 or Kir4.2 homomeric channels.

(Resubmitted 9 July 2001; accepted after revision 24 October 2001)
Corresponding author J. Teulon: INSERM U426, Faculté de Médecine Xavier Bichat, 16 rue Henri Huchard B.P. 416, 75870 Paris cedex 18, France. Email: teulon@bichat.inserm.fr

The distal convoluted tubule (DCT), a heterogeneous segment in most species, makes a moderate contribution to urine dilution and to the reabsorption of NaCl and calcium, and the secretion of potassium (Reilly & Ellison, 2000). Several studies have shown that massive K^+ conductance occurs across the basolateral membrane of this segment (Yoshitomi *et al.* 1989). As in other parts of the kidney, the K^+ conductance serves two purposes: it controls the membrane potential and recycles K^+ across the basolateral membrane. This latter function is essential for Na^+ absorption, which takes place in the DCT via a Na^+–Cl^- cotransporter and more distally via amiloride-inhibitable Na^+ channels. Na^+ enters the cell from the apical side and leaves from the basolateral side via Na^+,K^+-ATPase, where it is exchanged for K^+ ions. Adequate pump function is therefore dependent upon the ability of the K^+ conductance to adapt to the Na^+ load.

Using the patch-clamp technique, the K^+ channels in the basolateral membrane of the renal tubule have been studied mainly in the proximal tubule, where they have been shown to be inhibited by ATP (Wang *et al.* 1997). K^+ channels have also been described in the basolateral membrane of the cortical collecting duct (CCD), and it has been suggested that they may be regulated by cGMP (for a review, see Wang *et al.* 1997). In contrast, the K^+ channels in the DCT have not yet been investigated in detail, and a single rather preliminary study has reported the presence of a K^+ channel in the basolateral membrane of rabbit DCT (Taniguchi *et al.* 1989). In addition to these patch-clamp studies of renal tubule segments, the cloning of various K^+ channels has provided a mass of information about K^+ channels in the kidney, and especially about the ROMK (Kir1.1), the apically located inward rectifier K^+ channel that is involved in K^+ secretion in the CCD and in K^+ recycling across the thick ascending limb apical membrane (Wang *et al.* 1997). However, the correspondence between cloned K^+ channels and functionally described K^+ channels has generally not been established as far as channels located in the basolateral membrane are concerned. In a recent study, a Kir7.1 channel was immunolocalised at the

basolateral membrane of rat DCT (Ookata *et al.* 2000). This channel has a very low unitary conductance, which precludes single-channel recording (Krapivinsky *et al.* 1998). Another Kir channel, Kir4.1, is also present in the basolateral membrane of the rat DCT (Ito *et al.* 1996). This channel, the properties of which are known from studies involving the *Xenopus* oocyte expression system, can form complexes with Kir5.1 (Pessia *et al.* 1996; Tanemoto *et al.* 2000; Tucker *et al.* 2000), a subunit which *per se* has no channel activity (Bond *et al.* 1994). The Kir5.1 subunit has been shown to be present in the rat DCT, although the exact basolateral *versus* apical location has not been specified (Tucker *et al.* 2000). Evidence that another channel of the Kir4 family, Kir4.2, also reported to be present in the rat kidney (Shuck *et al.* 1997), forms a heteromeric channel with Kir5.1 has emerged very recently (Pessia *et al.* 2001).

In the present study, K^+ channels on the basolateral membranes of microdissected DCTs from the mouse kidney were investigated by means of the patch-clamp technique. We took particular care in characterising properties that could be used to compare these channels with native K^+ channels in the renal tubule on the one hand, and with cloned K^+ channels, particularly with Kir4.1 and Kir4.2 channels, on the other. Additionally, RT-PCR of microdissected DCTs was performed to investigate Kir4.1, Kir4.2 and Kir5.1 channels, and Kir4.1 was also investigated using immunohistochemical techniques. The K^+ inward rectifier channel reported here has functional properties compatible with Kir4.1–Kir5.1 and Kir4.2–Kir5.1 heteromeric channels, but not with Kir4.1 or Kir4.2 homomeric channels.

METHODS

Isolation of renal tubules

The experiments were carried out under licence no. 7427 of the Veterinary Department of the French Ministry of Agriculture. Male CD-1 mice (15–20 g, ICR according to the terminology of Harlan, Gannat, France) were killed by cervical dislocation. For patch clamping, the DCTs were isolated from the mouse kidneys after collagenase treatment (Worthington CLS II, 300 U ml^{-1}), as described previously (Teulon *et al.* 1987), except that L-15 Leibovitz medium (Eurobio, Les Ulis, France) was used throughout the tissue preparation procedure. Unlike rabbit DCT, mouse DCT is a heterogeneous structure composed of several types of cells (Reilly & Ellison, 2000). However, several studies have shown that the first section of the DCT (DCT1) consists mainly of distal cells, that possess the Na^+–Cl^- cotransporter (TSC), but not the epithelial sodium channel (see Reilly & Ellison, 2000). Consequently, in an attempt to patch mainly DCT1s, the patch-clamp recordings were done within the first loop of the DCT after the post-macula densa short thick ascending limb (TAL)-like segment. For the RT-PCR experiments, pools of isolated segments (3–6 isolated tubules, 0.2–0.5 mm long) from DCT were also microdissected from the kidney cortices of adult mice as described previously (Vandewalle *et al.* 1997).

Solutions and chemicals for the patch-clamp study

The tubules were initially bathed in physiological saline solution (PSS) containing (mM): 140 NaCl, 4.8 KCl, 1 $CaCl_2$, 1.2 $MgCl_2$, 10 glucose, 10 Hepes, adjusted to pH 7.4 with NaOH. Unless otherwise stated, the patch pipettes were filled with a high-K^+ solution containing (mM): 144.8 KCl, 1 $CaCl_2$, 1.2 $MgCl_2$, 10 glucose, 10 Hepes, adjusted to pH 7.4 with KOH. The high-K^+ solution (with Ca^{2+} and Mg^{2+}) was also used to superfuse the tubules when it was necessary to abolish the spontaneous membrane potential. Patches were excised from the DCTs into a high-K^+ solution, which contained no divalent ions and was supplemented with 5 mM EDTA. The solutions containing Mg^{2+} were usually supplemented with 2 mM EGTA. For experiments in which pH sensitivity was investigated, the pH of the solutions was adjusted with Hepes from 8.4 to 6.8, and with Mes to pH 6.4 and 6.6. We checked that the NP_o at pH 6.8 was similar when the patches were bathed with Hepes-buffered (NP_o = 8 ± 4 % of NP_o at pH 7.4, n = 4) or Mes-buffered (NP_o = 10 ± 4 % of NP_o at pH 7.4, n = 4) solutions.

Current recordings

Single-channel currents were recorded from patches of basolateral membranes using the cell-attached and excised, inside-out configurations of the patch-clamp technique (Hamill *et al.* 1981). Patch-clamp pipettes were pulled in two stages with a Kopf puller (Tujunga, CA, USA) using borosilicate glass (GC150T, Harvard Apparatus, Edenbridge, Kent, UK). They were coated with Sylgard and polished just before use. Currents were recorded with List LM-EPC7 or Bio-logic RK 400 patch-clamp amplifiers, monitored using Axoscope software (Axon Instruments, Foster City, CA, USA) and stored on digital audiotape (Sony DTR-1205, Bio-logic, Claix, France). In the cell-attached configuration, the clamp potential applied with respect to the bath (V_c) is superimposed on the spontaneous membrane potential, whereas in excised patches, it corresponds to the real transmembrane potential. V_c was corrected for liquid junction potentials as described elsewhere (Barry & Lynch, 1991). The liquid junction potentials were also measured directly as described previously (Teulon *et al.* 1987). As usual, currents resulting from the movement of cations from the inner to the outer face of the patch membrane were considered to be positive and are shown as upward deflections in the current tracings. The experiments were carried out at room temperature (22–27 °C).

Data analysis

Single-channel current recordings were filtered at 700 Hz low-pass using an 8-pole Bessel filter (LPBF-48DG, NPI Electronic, Tamm, Germany) and digitised at a sampling rate of 3 kHz using a Digidata 1200 analog-to-digital converter and Axoscope software (Axon Instruments). Channel activity was measured from digitised stretches of recording lasting at least 30 s using custom-built software (T. Van Den Abbeele, Paris, France). The principle of this software was as follows. The time-averaged current passing through the channels on the patch ($<I>$) was calculated from current amplitude histograms, taking the closed current level as reference. NP_o and P_o were estimated from the equation: $<I> = NP_o i$, where N, P_o and i are the number of channels in the patch, the open state probability and the amplitude of the unitary current, respectively. The maximum number of channels open simultaneously was determined by a visual inspection of the whole recording in order to calculate P_o. The P_o values obtained in this way were 100.8 ± 1.4 % and 97.4 ± 24 % of the P_o obtained with the Pstat (pCLAMP 8, Axon Instruments) and Tac (Bruxton, Seattle, USA) softwares, respectively (n = 6).

The unitary conductance was measured as a slope conductance for inward currents (g_{in}) and as a chord conductance (at a specified potential) for outward currents (g_{out}) when inward rectification was present. The reversal potentials (E_r) were deduced from linear regression of the experimental data points over the linear part of the i–V_c relationships. Specifically, for cell-attached patches in PSS, g_{in} was calculated by means of linear regression of data points between −80 mV and +60 mV ($[K^+]$ = 15, 40 and 145 mM; Fig. 2*A*) or −20 mV and +100 mV ($[K^+]$ = 400 mM; Fig. 2*A*) and E_r was extrapolated from this fit (Fig. 1*B*). It was not always possible to record currents beyond the reversal potential. To determine the ion selectivity in cell-attached patches (see Fig. 2*B*), the E_r values were interpolated from linear regression of data points between −90 mV and +10 mV. For cell-attached patches in high-K^+ solution (Fig. 1*B*) or excised patches in symmetrical high-K^+ solutions (Fig. 4*B*), g_{in} was calculated over the −80 mV to −10 mV range.

The permeability ratio, P_{Na}/P_K, was estimated for the cell-attached and excised patches. In cell-attached patches, i–V_c relationships were established from separate patches for three different pipette K^+ concentrations ($[K^+]_p$) after the resting membrane potential had been abolished by superfusion of a high-K^+ solution. E_r values were corrected for junction potentials which varied from 4 mV for $[K^+]_p$ = 145 mM to 0.3 mV for $[K^+]_p$ = 15 mM. The plot of reversal potential against $[K^+]_p$ was fitted to the Goldman-Hodgkin-Katz voltage equation, taking E_r obtained with 145 mM K^+ in the pipette as reference. This gave an estimate of P_{Na}/P_K. The following equation was used:

$$E_r = \frac{RT}{F}\ln\frac{P_K[K^+]_p + P_{Na}[Na^+]_p}{P_K[K^+]_i} = \frac{RT}{F}\ln\left([K^+]_p/C + \frac{P_{Na}}{P_K}\left(1 - [K^+]_p/C\right)\right), \quad (1)$$

with $[Na^+]_p + [K^+]_p = [K^+]_i = C$ = 144.8 mM, where subscripts p and i refer to the pipette and the intracellular sides of the patch, respectively, and R, T and F have their usual meanings. We assumed that DCT cells superfused with high-K^+ solution had negligible $[Na^+]_i$.

In excised patches, i–V_c relationships were established in the presence of a solution containing 130 mM NaCl and 15 mM KCl (glucose and Hepes as in PSS, no Ca^{2+}, EGTA added), using pipettes filled with the high-K^+ solution. The internal solution was Mg^{2+} free in order to eliminate the rectifying effect of this divalent cation. Since in most cases it was impossible to measure currents accurately beyond the reversal potential, an estimate of P_{Na}/P_K was derived by fitting the experimental data points to the current equation of Goldman-Hodgkin-Katz. The following equation was used:

$$i = \frac{\left(0.001GV_c\left(\frac{[K^+]_i}{[K^+]_p} + \frac{P_{Na}}{P_K}\frac{[Na^+]_i}{[K^+]_p} - \exp(-F/RT)\right)\right)}{1 - \exp(-F/RT)}, \quad (2)$$

where

$$G = \frac{P_K F^2}{RT}[K^+]_p.$$

G is the unitary conductance in symmetrical conditions for $[K^+]$ = 145 mM. The factor 0.001 was introduced for unit consistency (i in pA, G in pS and V_c in mV).

RT-PCR analysis

Total RNA was extracted from microdissected DCTs using the RNA-PLUS extraction kit (Bioprobe Systems, Montreuil-sous-Bois, France), and treated with ribonuclease-free deoxyribonuclease I (Boehringer, Manheim, Germany) at 37 °C for 30 min. The RNA was reverse-transcribed using Moloney murine leukaemia virus reverse transcriptase (Life Technologies, Eragny, France) at 42 °C for 45 min. Microdissected tubule cDNA was amplified for 30–32 cycles in a total volume of 100 μl of PCR buffer (50 mM KCl, 20 mM Tris-HCl, pH 8.4) containing 1.5 mM $MgCl_2$, 40 μM dNTP, 1 μCi [α-^{32}P]dCTP, 1 U *Taq* polymerase, 7.5 pmol Kir4.1 and 18 pmol hGAPDH primers or 7.4 pmol Kir4.2 and 21.5 pmol hGAPDH primers or 7 pmol Kir5.1 and 29 pmol hGAPDH primers. The following primers were used.

Kir4.1: sense, 5′-TATCTGGTAGCTGTGGCCCATG-3′
and antisense, 5′-AGATCGCAGGCGTGAACTCGT-3′.
Kir4.2: sense, 5′-GTTCAGCCACTGTGCTGTCATC-3′
and antisense, 5′-TGGAGAGAGAAACCACAGGCAC-3′.
Kir5.1: sense, 5′-GCTATCCTCCAGAGCATGCCATC-3′
and antisense, 5′-AGTCACCTATGCGCCACATGAGGCA-3′.

The hGAPDH (glyceraldehyde-3-phosphate dehydrogenase) primers, used as an internal standard, were the same as those described by Hummler *et al.* (1996). The temperature cycling programme was as follows: 94 °C for 30 s, 55 °C for 30 s, and 72 °C for 1 min. The amplification products were run on 4% polyacrylamide gels and autoradiographed. The sets of Kir4.1, Kir4.2 and Kir5.1 primers yielded amplified products of the expected size. We checked that no amplification products could be detected under control conditions using non-reverse-transcribed RNA extracted from microdissected DCTs. In addition, sequence analysis of PCR products confirmed that they matched the expected cDNA analyses (data not shown).

Immunohistochemical studies

Mice were killed by intraperitoneal injection of an overdose of sodium pentobarbital, and the kidneys were rapidly removed, cut along the longitudinal axis of the medullary rays, and immediately frozen in liquid nitrogen and stored at −80 °C until use. Frozen kidney sections (7–9 μm) mounted on glass slides and fixed in ice-cold methanol for 8 min were incubated with a rabbit anti-rat Kir4.1 antibody (1:200 dilution) (Ito *et al.* 1996) overnight at 4 °C. After being rinsed in phosphate-buffered saline (PBS), samples were incubated with goat anti-rabbit Ig coupled to either Alexa Fluor 488 (Al 488, 1:500) or Cy3 (1:200) fluorescent dyes (Jackson Immunoresearch, West Grove, PA, USA) for 1 h at room temperature. The nuclei were also counterstained with Sytox (1:500; Molecular Probes Europe BV, Leiden, The Netherlands).

Tissue sections were also double-labelled using the anti-Kir4.1 antibody and a polyclonal antibody directed against the thiazide-sensitive Na^+–Cl^- cotransporter (TSC, 1:500) (Plotkin *et al.* 1996, kindly provided by S. C. Hebert). Samples were incubated with the anti-Kir4.1 antibody as described above, rinsed with PBS, and incubated for 30 min or 1 h at room temperature with the anti-TSC antibody. Binding was detected with Fab goat anti-rabbit Ig (1:50; Jackson Immunoresearch). All tissue sections were examined by confocal laser scanning microscopy (CLSM) (Leica, Wetzlar, Germany).

Statistics

Results are given as means ± S.E.M. for the indicated number of measurements (n). Origin software (Microcal, Northampton, MA, USA) was used to fit the data points to equations. Statistical

significance was evaluated by Student's *t* test or one-way analysis of variance and Student-Newman-Keuls method (subconductance levels). $P < 0.05$ was considered significant.

RESULTS

Channel activity in cell-attached patches

Two types of channels were detected when cell-attached patches were formed on the basolateral membranes of DCTs bathed with PSS, using the high-K^+ solution in the pipette. One channel, with a conductance of 25–30 pS, was detected in about 20 % of patches, and had a linear current–voltage relationship. This channel was not a K^+ channel: E_r and g values determined using pipettes filled with high-K^+ solution were not statistically different from those determined with PSS-filled pipettes (high-K^+ solution: $E_r = 66.3 \pm 5.8$ mV and $g = 27.0 \pm 2.5$ pS, $n = 4$; PSS: $E_r = 56.4 \pm 7.2$ mV and $g = 24.2 \pm 1.2$ pS, $n = 5$). This channel resembled a non-selective cation channel previously reported from our laboratory (Chraïbi *et al.* 1994). Another channel appeared to be abundantly present in the DCT. It was found in about 50 % of patches (57 out of 115 patches) and each patch contained between one and 12 such channels (mean: 4.6 channels per patch). Figure 1*A* shows typical excerpts of single-channel recordings at various voltages for a cell-attached membrane patch (high-K^+ solution in the pipette) that contained six channels of the same type. The mean current–voltage relationship was roughly linear for voltages less positive than E_r, but clearly deviated from linearity at more positive voltages (Fig. 1*B*). This suggests that the channel is of the inwardly rectifying type. The inward slope conductance was 40.4 ± 1.2 pS ($n = 6$). The reversal potential (72.1 ± 2.4 mV, $n = 6$) was close to the expected value for a cation channel under these conditions. It is apparent from the channel currents in Fig. 1*A* that channel activity decreased at positive clamp potentials. This was typically observed in five patches in which the voltage dependence was investigated: the open state probability (P_o) remained stable over the interval −80 mV to 0 mV and decreased at higher potential values (Fig. 1*B*, inset). P_o at +40 mV was about one-third as great as that at 0 mV.

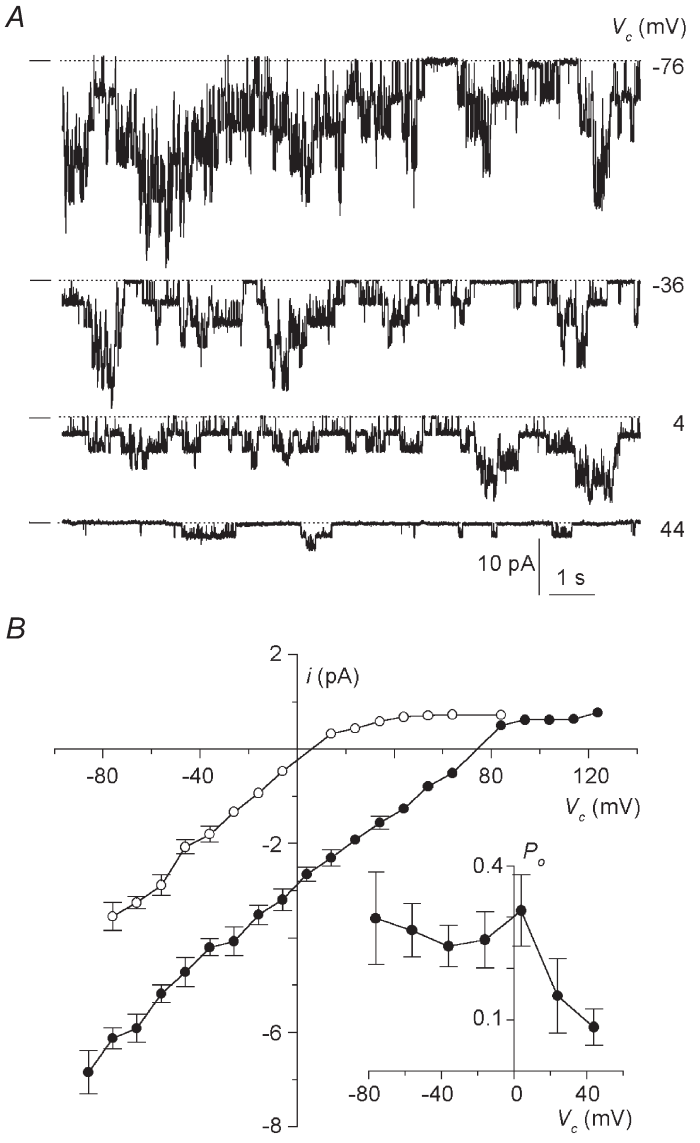

Figure 1. Channel activity in the cell-attached configuration

A, representative current recordings from a membrane patch formed on a DCT bathed with physiological saline solution (PSS; high-K^+ solution in the pipette), at various clamped potentials (V_c, as indicated to the right of each trace). The dashed line in this and subsequent figures denotes the closed current level. *B*, mean single-channel current (i)–voltage (V_c) relationships obtained with the pipette containing the high-K^+ solution and the bath, either PSS (140 mM NaCl, 4.8 mM KCl, ●) or high-K^+ solution (○). With the high-K^+ solution, the resting membrane potential was close to zero. Each point shown is the mean of 3–12 determinations from 12 separate patches. S.E.M. values are shown as error bars when they are larger than the symbols. Inset: voltage dependence. P_o is plotted against V_c (each point is the mean of 3–5 values obtained from 5 separate patches).

Inward rectifying currents were further studied on DCTs superfused with the high-K^+ solution (Fig. 1*B*). This made it possible to compare the inward and outward conductances in a more straightforward way, since E_r was close to zero (4.7 ± 0.6 mV, $n = 8$). The mean inward slope conductance (g_{in} = 43.3 ± 2.1 pS, $n = 8$) was considerably higher than the chord conductance for outward currents (g_{out} = 9.0 ± 0.4 pS, $n = 4$) measured between E_r and +80 mV. The ratio g_{in}/g_{out} (4.7 ± 0.4, $n = 4$) points to intermediate inward rectification.

Lowering the concentration of K^+ in the pipette reduced the inward conductance. The inward conductances were measured as the slope conductance in cell-attached patches bathed with normal PSS, and plotted against the K^+ concentration in the pipette (Fig. 2*A*). The data points could be empirically fitted to a Michaelis-Menten equation (Mauerer *et al.* 1998*a*). A maximal conductance of 48 pS and K_m of 65 mM were obtained.

The ion selectivity of the channel was investigated in the cell-attached configuration on DCTs superfused with high-K^+ solution, using three different K^+ concentrations in the pipette. The E_r values were plotted against the K^+ concentration in the pipette (Fig. 2*B*) and fitted to the Goldman-Hodgkin-Katz current equation (see Methods). A P_{Na}/P_K permeability ratio of 0.1 was obtained.

The results obtained in the cell-attached configuration identify a classical inwardly rectifying K^+ channel as the major K^+ channel of the DCT basolateral membrane in the resting state.

Current sublevels

Brief subconductance levels occurred consistently in the DCT K^+ channels of cell-attached patches (Fig. 3). They were difficult to analyse because (i) most of the recordings were from multichannel patches and (ii) the sub-conductance levels made too small a contribution to the open current to allow discriminating all-point amplitude histograms to be constructed. We therefore isolated stretches of data from cell-attached patches at a V_c of 0 mV which had only one channel active ($n = 7$) and measured the current amplitudes using the averaging cursor facility of Axoscope software. Three significantly different sublevels, S_1, S_2 and S_3, were detected with amplitudes 0.29 ± 0.02 ($n = 7$), 0.48 ± 0.03 ($n = 6$) and 0.71 ± 0.02 ($n = 7$) as great as the fully open amplitude. This is illustrated in Fig. 3. The contribution of each sublevel to the overall open current was very limited: the channels spent 0.5 ± 0.1 % of the total open time at S_1, 0.6 ± 0.3 % at S_2 and 1.2 ± 0.3 % at S_3.

Channel rundown and ion selectivity in excised patches

Channel activity was lost within minutes when the membrane patch was excised in normal PSS (containing millimolar concentrations of Mg^{2+} and Ca^{2+}). In contrast, no rundown was detected when the DCTs were exposed to a high-K^+ solution containing no Mg^{2+} or Ca^{2+} (5 mM EDTA added) *prior* to excision. For instance, the NP_o measured 3–4 min after excision over 1 min was 108 ± 3 % of the initial NP_o ($n = 4$). This pre-exposure to a high-K^+ solution procedure was used routinely for most experiments on excised patches.

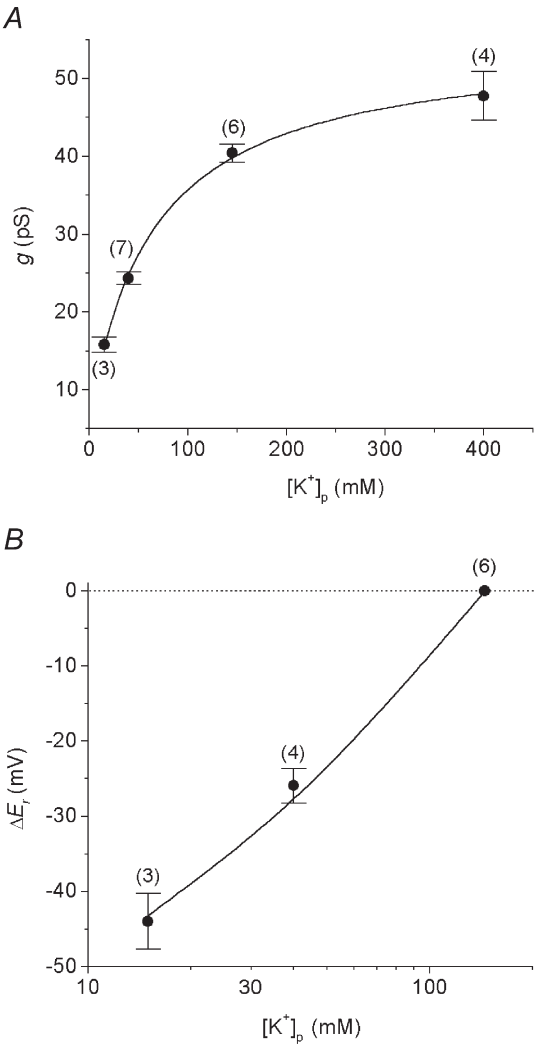

Figure 2. Conductance and ion selectivity in the cell-attached configuration

A, channel conductance (g) as a function of the concentration of K^+ in the pipette ($[K^+]_p$ = 15, 40, 144.8 and 400 mM). g was measured in cell-attached patches bathed with PSS through regression of the data points over the linear part of the i–V_c curve (see Methods for details). The relationship between g and $[K^+]_p$ was described by the equation: $g = g_{max}(1 + K_m/[K^+]_p)^{-1}$. K_m = 65 mM, g_{max} = 48 pS. *B*, channel ion selectivity determined in the cell-attached mode by varying the concentration of K^+ in the pipette. Relative reversal potentials (ΔE_r) are plotted as a function of $[K^+]$ in the pipette ($[K^+]_p$) on a logarithmic scale. ΔE_r are mean values measured from individual i–V_c relationships (see Methods). The reversal potential with 145 mM K^+ in the pipette was taken as reference. The line is a non-linear fit to the Goldman-Hodgkin-Katz equation with P_{Na}/P_K = 0.1. The numbers in parentheses indicate the number of observations.

We checked that the K^+ selectivity of the channel measured in excised patches was similar to that estimated in cell-attached patches by exposing the intracellular side of the patch to a 130 mM NaCl solution containing no Mg^{2+} or Ca^{2+} (EDTA added). The resulting i–V curve, fitted to the Goldman-Hodgkin-Katz equation (see Methods, not shown), yielded a P_{Na}/P_K of 0.11 ± 0.02 (n = 7).

Block by external barium

External Ba^{2+} blocked channel activity in outside-out patches bathed with high-K^+ solutions on both sides. The bath contained Mg^{2+} (1.2 mM) and Ca^{2+} (1 mM), and the pipettes were filled with a Mg^{2+}-free solution (EDTA added) to avoid channel rundown. Ba^{2+} at concentrations of 10^{-5}, 10^{-4} and 10^{-3} M reduced NP_o to 87 ± 6, 33 ± 9 and 5 ± 2 % of control, respectively (n = 3).

Effects of internal Mg^{2+} and spermine on conduction properties

It is recognised that intracellular Mg^{2+} is responsible for inducing inward rectification of unitary channel currents. We confirmed that this was also true of the DCT channel by establishing i–V relationships in the nominal absence of Mg^{2+} (EDTA added) and presence of 1.2 mM Mg^{2+}. The results, shown in Fig. 4*A* and *B*, demonstrate that the i–V_c relationship was linear in the nominal absence of Mg^{2+} (g = 35.4 ± 2.9 pS, g_{in} not different from g_{out}: P = 0.8, n = 7), and displayed inward rectification in the presence of 1.2 mM Mg^{2+}. In the presence of Mg^{2+}, the inward conductance did not differ from control (P = 0.7, g_{in} = 34.2 ± 2.6 pS, n = 8), whereas the outward conductance, estimated as the chord conductance at 80 mV, was significantly different ($P < 0.001$ *vs.* control, g_{out} = 8.1 ± 1.8 pS, n = 5), giving a g_{in}/g_{out} ratio of 4.8 ± 0.8 (n = 5). The data were described using the following equation, according to the model originally derived by Woodhull (1973):

$$\frac{I_{Mg}}{I_{0Mg}} = \frac{gV}{1 + [Mg^{2+}]/K_0 \exp(2FV\delta/RT)},$$

where V is the voltage across the membrane, δ represents the 'electrical distance' of the binding site from the outside of the channel pore, K_0 is the concentration causing a 50 % decrease in unitary current at 0 mV, and F, R and T have their usual meanings. The best fit of the data yielded δ = 0.31 ± 0.06 and K_0 = 2.3 ± 0.9 mM.

When the tetravalent cation spermine is applied intracellularly it induces a voltage-dependent block of several inwardly rectifying K^+ channels. This blockade manifests itself by the reduction of P_o at negative voltages and macroscopic inwardly rectifying currents. Spermine (5×10^{-7} M) decreased NP_o to 46 ± 5 % of control at +60 mV (n = 4), but had no impact at −60 mV (NP_o = 102 ± 6 % of control, n = 6). Spermine had almost no effect at 5×10^{-8} M (NP_o = 84 ± 5 % of control, n = 4) at +60 mV.

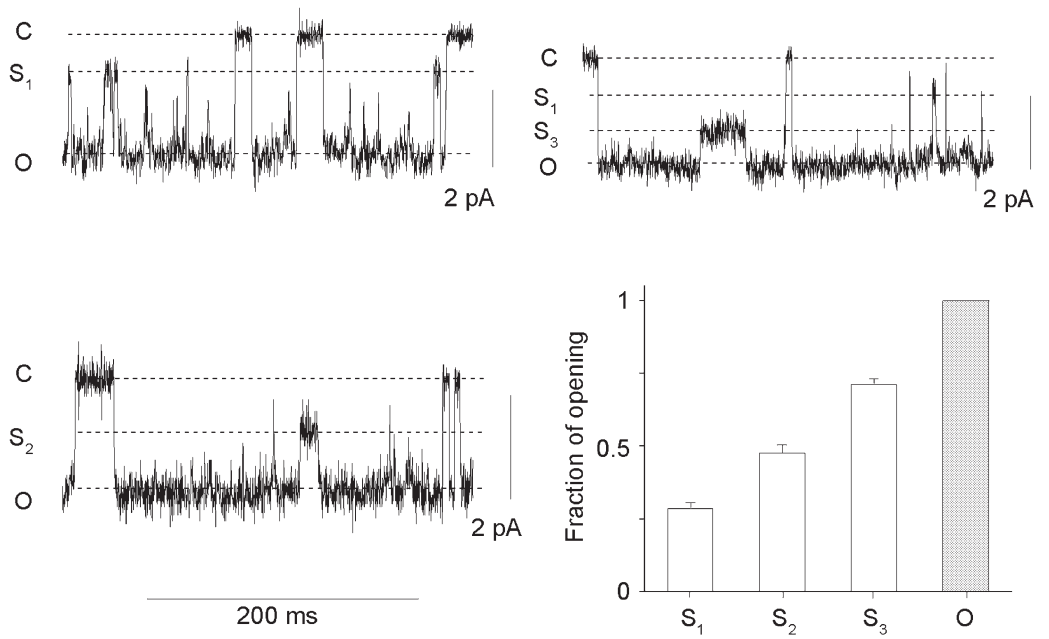

Figure 3. Subconductance levels of the DCT K^+ channel

Short excerpts of channel current traces recorded from 3 separate cell-attached patches at 0 mV are shown. C, S_1, S_2, S_3 and O denote the closed level, the first, second and third subconductance levels and complete opening, respectively. Mean data are shown in the histogram. The sublevel current values in each recording were derived from 2–13 averaging measurements. The total open time in these recordings ranged between 2.3 and 17.0 s. S_1, S_2 and S_3 subconductance levels were significantly different from each other (one-way analysis of variance and Student-Newman-Keuls method).

Effects of internal pH, Ca^{2+} and ATP on channel activity

We examined the effects of intracellular pH in inside-out membrane patches, which were bathed with nominally Mg^{2+}-free solutions to keep the channel activity constant. Changing the intracellular pH over the range 6.4–8.4 affected channel activity, a decrease in pH reducing, and conversely an increase in pH elevating, P_o. The effect was fully reversible (not shown). Figure 5*A* shows examples of channel currents recorded at three different pH values from an inside-out patch that contained seven channels. The mean relationship between NP_o and pH is given in Fig. 5*B*, where the data were fitted to a Hill equation. The pK_a was calculated to be 7.6. The changes in pH_i had no impact on the current amplitude.

The possible effects of intracellular Ca^{2+} were investigated. Interference from Ca^{2+}-activated non-selective cation channels (Chraïbi *et al.* 1994) was avoided by using Mg^{2+}-free PSS (no EDTA added) and recording K^+ channel activity at 0 mV. Increasing $[Ca^{2+}]_i$ from 10^{-9} M to 10^{-5}, 10^{-4} or 10^{-3} M did not affect channel activity. NP_o, expressed as a percentage of NP_o at 10^{-9} M Ca^{2+}, was 97 ± 8 % at 10^{-5} M Ca^{2+}, 97 ± 6 % at 10^{-4} M Ca^{2+} and 86 ± 6 % at 10^{-3} M Ca^{2+} ($P > 0.1$, data not shown, $n = 4$). Exposing inside-out patches to high intracellular Ca^{2+} (10^{-3} M) for about 2–3 min induced only minor channel rundown, since the subsequent NP_o measured at 10^{-9} M Ca^{2+} was 77 ± 8 % of the initial NP_o at 10^{-9} M Ca^{2+} ($P = 0.01$, not shown, $n = 3$).

Several K^+ channels in the renal tubule can be inhibited by millimolar concentrations of intracellular ATP. We tested the effects of 2 mM ATP on the DCT channel by measuring NP_o before, during and after perfusion of ATP and expressing the results as a percentage of NP_o of the two controls. In a first series of experiments, high-K^+ solution containing no divalent cations (supplemented with EDTA) was used; in the presence of ATP, NP_o was 113 ± 10 % of the control value ($n = 4$). In a second series of experiments, high-K^+ solution containing 1.2 mM free Mg^{2+} (2 mM EGTA added) was used, and in the presence of ATP, NP_o was 95 ± 10 % of control ($n = 4$). Internal ATP therefore had no inhibitory effect on channel activity.

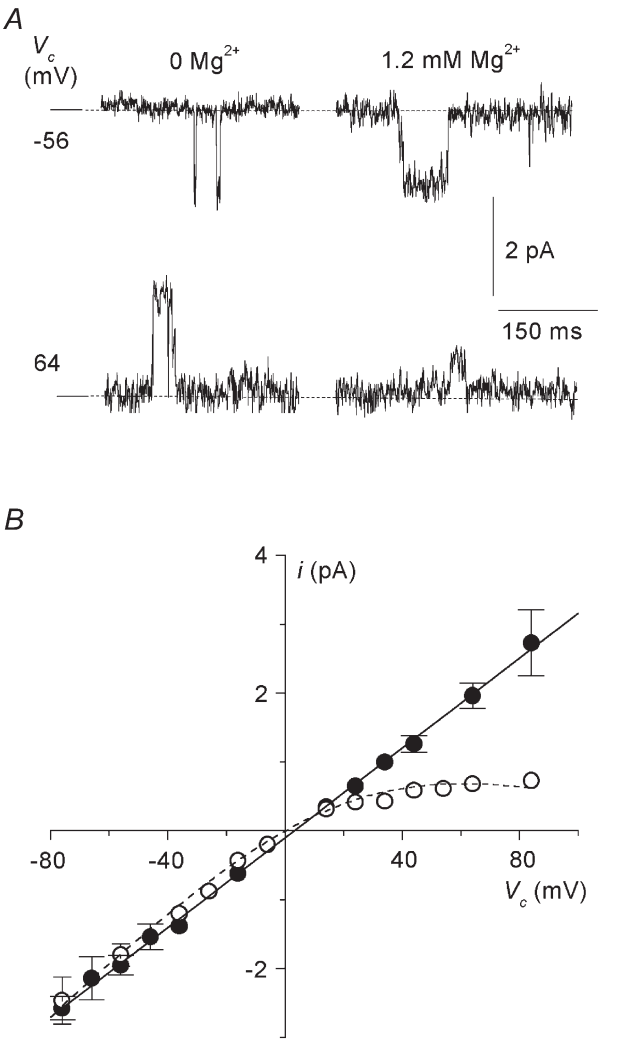

Figure 4. Effect of Mg^{2+} on the current–voltage relationship

A, short excerpts of single-channel recordings showing the amplitude of channel openings at −56 and +64 mV in the nominal absence and in the presence of 1.2 mM Mg^{2+}. Current amplitude was considerably reduced in the presence of 1.2 mM Mg^{2+} at positive voltages. *B*, mean i–V_c relationships in the presence (○) and absence (●) of Mg^{2+}. The relationship in the presence of Mg^{2+} was fitted to the equation as described in the text ($g = 36.1 \pm 2.8$ pS, $K_0 = 2.3 \pm 0.9$ mM, $\delta = 0.31 \pm 0.06$). The results were obtained from 10 patches ($n = 3$–10 for each data point).

Channel rundown induced by internal Mg^{2+}

Besides inducing inward rectification, Mg^{2+} gradually and irreversibly decreased channel activity in inside-out patches. The channel recording shown in Fig. 6*A* was obtained from a highly active inside-out patch that contained 14 K^+ channels. The patch, initially bathed with a Mg^{2+}-free solution containing EDTA (not shown), was subsequently exposed first to a nominally Mg^{2+}-free solution (2 mM EGTA added), which barely altered the channel activity, and then to the same solution supplemented with 1.2 mM Mg^{2+}. In the presence of Mg^{2+}, NP_o gradually fell to 40 % of control after perfusion for 1 min and then to less than 5 % of control after 3 min. Similar observations were made on a total of 11 patches. The averaged time course of the decrease in channel activity upon exposure to Mg^{2+} is shown in Fig. 6*C*, where NP_o values from sequential 30 s stretches of data (as a percentage of control) are plotted against time. On average, NP_o fell by one-half in 1 min, and was less than 10 % of control after 4 min exposure to Mg^{2+}. The decrease in NP_o was not reversible when Mg^{2+}-free solution was reperfused (see Fig. 6*A*, and the shaded bars at 5–6 min in Fig. 6*C*).

In separate experiments, we recorded channel activity in the absence of Mg^{2+} (EDTA added) for a comparable period ($n = 8$ patches). As illustrated in Fig. 6*B*, NP_o in the absence of Mg^{2+} remained relatively unchanged over this period of time. On average, NP_o was 100 ± 13 % of control after 3 min of recording in Mg^{2+}-free solution (see Fig. 6*C*, open circles) *versus* 14 ± 5 % in the presence of Mg^{2+} at the same time. At the end of this period, the same patches were exposed to a solution containing 1.2 mM Mg^{2+}. A decline in channel activity was then observed (see Fig. 6*B*), which on average, was faster, but less pronounced, than that in the previous experiments (Fig. 6*C*, filled circles).

Expression of mRNA for Kir4.1, Kir4.2 and Kir5.1 channels in DCT cells

RT-PCR was performed on microdissected mouse DCTs to study the expression of Kir4.1, Kir4.2 and Kir5.1 (Fig. 7). Substantial amounts of transcripts for the three channels

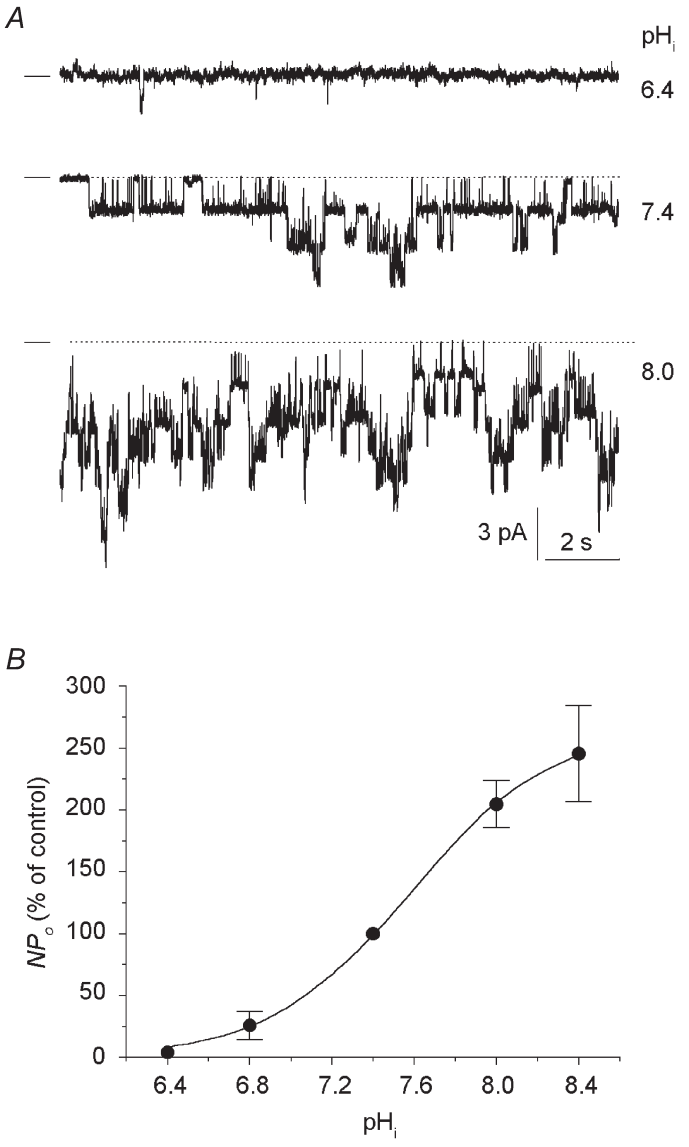

Figure 5. Effects of intracellular pH on K^+ channel activity

A, channel current traces showing that channel activity decreased at an acid pH, and increased at an alkaline pH. The recording was done at −50 mV in the inside-out configuration using high-K^+ solutions on both sides of the patch, with no Mg^{2+} on the internal side. The value of the intracellular pH (pH_i) is indicated to the right of each trace. No decrease in channel amplitude was apparent. *B*, dose–response curve for the effects of pH_i on channel activity expressed as a percentage of NP_o at pH 7.4. The curve is the best fit of the experimental points to the equation: $NP_o = NP_{o,max}/\{1 + ([H^+]/K)^{n_H}\}$, where K is the proton concentration causing 50 % inhibition ($pK_a = 7.6$) and n_H is the Hill coefficient ($n_H = 1.3$). Each data point is the mean of 6–8 measurements (8 patches).

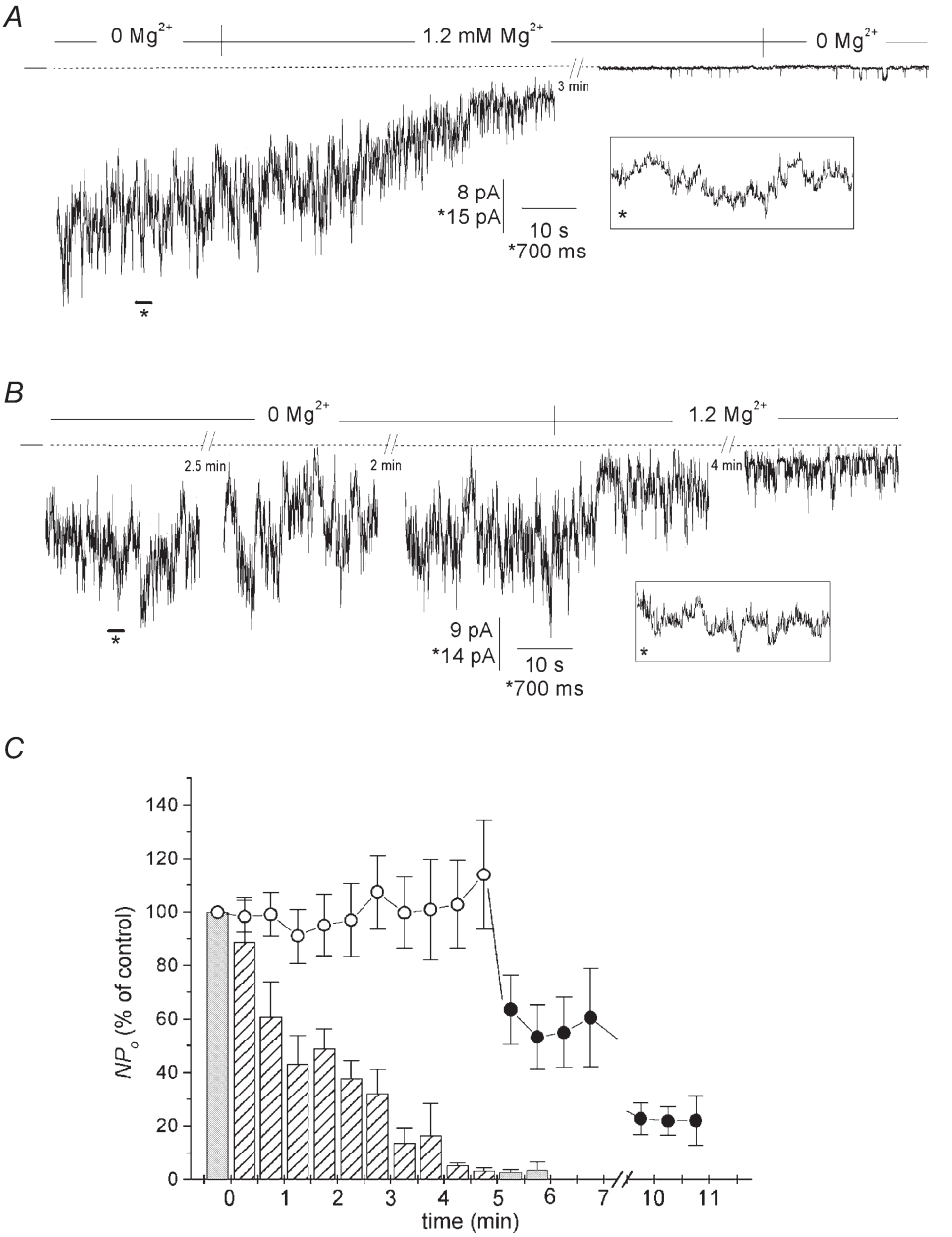

Figure 6. Inhibitory effect of Mg^{2+} on K^+ channel activity

Channel current traces in *A* and *B* are from 2 separate inside-out patches symmetrically bathed with high-K^+ solution. *A*, exposure of this patch membrane to 1.2 mM Mg^{2+} induced a gradual decrease in NP_o, which eventually resulted in the almost total disappearance of channel activity in this particular example. Removal of Mg^{2+} did not restore channel activity. Inset: a brief excerpt of the recording (indicated by the asterisk) is shown on an expanded time scale. *B*, this patch was exposed first to a Mg^{2+}-free solution (EDTA added) for 5 min and then to solution containing 1.2 mM Mg^{2+}. No channel rundown was apparent in the absence of Mg^{2+}. *C*, channel activity in the presence and absence of Mg^{2+}. The histograms show the average time course of channel activity in the presence (bars) or absence (circles) of Mg^{2+} for two experimental series. For the first series, NP_o in the presence of Mg^{2+} (hatched bars) was measured in individual current recordings for sequential 30 s stretches of data and is expressed as a percentage of control NP_o (NP_o in the absence of Mg^{2+}, shaded bar at time zero). Reperfusion of a Mg^{2+}-free solution did not restore channel activity (shaded bars at 5–6 min). Each bar is the mean of 3–11 values (11 patches). For the second series, NP_o in the absence of Mg^{2+} (○) was measured under the same conditions and is expressed as a percentage of control NP_o (NP_o at time zero). Exposure to Mg^{2+} induced a rapid decrease in channel activity (●). Each point is the mean of 3–8 values (8 patches).

were detected, compared with the amount of GAPDH transcript, which was used as an internal standard (Fig. 7).

Immunolocalisation of Kir4.1 channel in DCT cells

Indirect immunofluorescence studies showed that some tubule sections of the mouse kidney cortex were intensely labelled by the anti-Kir4.1 antibody (Fig. 8*A*). Some of the Kir4.1-positive tubule sections were stained by an antibody raised against the thiazide-sensitive Na^+–Cl^- cotransporter (TSC) expressed in DCT cells (Fig. 8*A*). This indicates that Kir4.1 co-localises with this cotransporter, which is specific to DCT1. To determine the subcellular distribution of Kir4.1 more precisely, sections were labelled with the Kir4.1 antibody and counterstained with Sytox to identify the nuclei (Fig. 8*B*). DCT cells exhibited an intense staining delineating the basal peripheries of the cells, and an intracytoplasmic staining restricted to the basal side of the cells, which could have been due to the numerous enfoldings of the basolateral membranes (Fig. 8*B*).

DISCUSSION

On investigating basolateral K^+ channels at the single-channel level in the DCT, we observed a single type of K^+ channel, which appeared to be abundantly expressed. The main properties exhibited by the channel are Mg^{2+}-induced inward rectification, blockade by internal spermine or external barium, sensitivity to pH and insensitivity to ATP.

Inward rectification properties of the DCT K^+ channel

Inward rectification can be classified as 'strong' to 'mild' (Nichols & Lopatin, 1997). As far as we know, renal K^+ channels only display 'mild' to 'intermediate' inward rectification. The low-conductance K^+ channel in the TAL and CCD apical membranes clearly displays modest inward rectification, since a rectification coefficient (g_{in}/g_{out}) of 2.3 can be deduced from published data (Wang *et al.* 1990). We calculated higher g_{in}/g_{out} coefficients of ~4–6 for basolateral K^+ channels in the proximal tubule of various species (Hunter, 1991; Beck *et al.* 1993; Mauerer *et al.* 1998*a*) and in rabbit cortical thick ascending limb (CTAL) (Hurst *et al.* 1992). The basolateral DCT K^+ channel has a similar g_{in}/g_{out} (~4.7) and, in addition, opening can be observed at potentials beyond the reversal potential, a feature not observed for strong inwardly rectifying K^+ channels. Thus the DCT K^+ channel can be defined as an 'intermediate' inward rectifier.

Our results indicate that Mg^{2+}-induced rectification of the DCT K^+ channel resembles that of 'mild' inwardly rectifying K^+ channels (Nichols & Lopatin, 1997). The computed concentration of Mg^{2+} causing a 50 % decrease in unitary current at 0 mV (K_0) was 2.3 mM, which is lower than the only published value for native renal K^+ channels (K_0 = 7.7 mM; Mauerer *et al.* 1998*a*), but similar to that for the native ATP-dependent K^+ channel in heart ventricular cells (~2 mM; see Matsuda, 1991*b*) or the cloned Kir1.1 channel (2–13 mM; Nichols *et al.* 1994; Taglialatela *et al.* 1995). This value is considerably higher than the K_0 of about 10 μM reported for the strong inward rectifiers (Matsuda, 1991*b*; Taglialatela *et al.* 1995; Yamashita *et al.* 1996). Another feature that this channel shares with mild inward rectifiers (Matsuda, 1991*b*; Nichols *et al.* 1994) is the estimated electrical distance 'sensed' by Mg^{2+} (estimated to

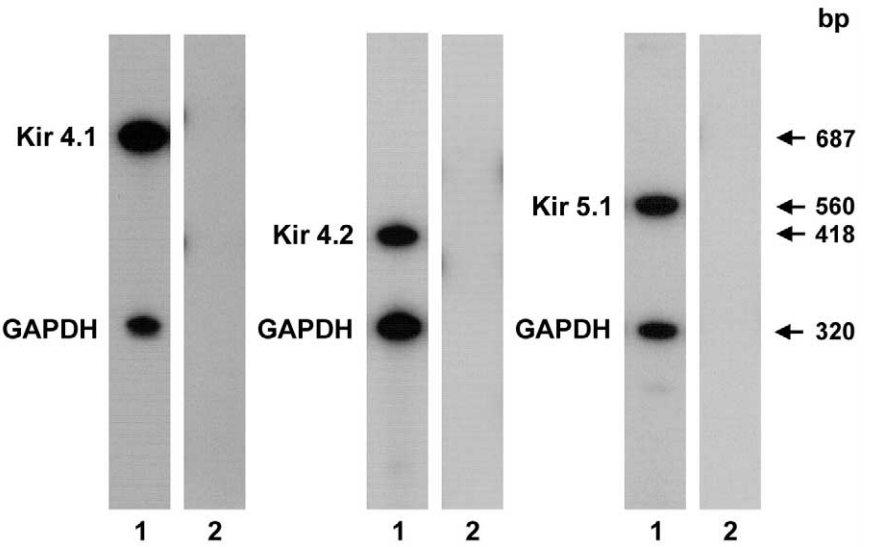

Figure 7. Kir4.1, Kir4.2 and Kir5.1 mRNA expression in the mouse DCT

RT-PCR was performed on cDNA extracted from microdissected DCTs. Each sample was amplified with sets of primers specific for Kir4.1 (32 cycles), Kir4.2 (30 cycles) and Kir5.1 (30 cycles) and internal standard hGAPDH primers. The sets of primers used yielded amplified products of the expected size (lanes 1: Kir4.1, 687 bp; Kir4.2, 418 bp; Kir5.1, 560 bp; GAPDH, 320 bp). No amplified products (lanes 2) were detected when non-reverse-transcribed RNAs were amplified.

be about 0.3 for the DCT K^+ channel), which contrasts with that of strong inward rectifiers (δ ~0.6; Matsuda, 1991*a*; Wible *et al.* 1994).

At a concentration of 5×10^{-7} M, spermine reduced P_o by 50 % at positive voltages. This property has not been investigated for any other kidney K^+ channels, except in the ambystoma proximal tubule where spermine had no effect (Mauerer *et al.* 1998*a*). Typical weakly inward rectifiers are barely sensitive to this agent, since the concentration causing one-half of the maximum inhibition (IC_{50}) is about 10^{-3} M (Wible *et al.* 1994) for the cloned Kir1.1, whereas the IC_{50} concentrations for the native muscarinic K^+ channel (Yamada & Kurachi, 1995) or cloned Kir2.1 or Kir4.1 are in the 10^{-8} M range (Fakler *et al.* 1994). The corresponding value for the DCT channel is tenfold higher than the IC_{50} for Kir4.1, but considerably lower than the IC_{50} observed for Kir1.1. Thus the DCT K^+ channel has intermediate spermine blocking properties. In cloned K^+ channels (homotetramers), it is accepted that the sensitivity to spermine correlates with the sensitivity to fast Mg^{2+} block (Nichols & Lopatin, 1997). However, it has been shown (Glowatzki *et al.* 1995) that heterotetramers formed by strong and mild inward rectifiers have intermediate properties with regard to their sensitivity to spermine.

Comparison with other kidney K^+ channels

The only previous patch-clamp study on basolateral K^+ channels in the DCT was done in the rabbit and reported voltage-independent, Ba^{2+}-sensitive channels with slightly higher unitary conductance values of 49–60 pS (Taniguchi *et al.* 1989). Inward rectification and sensitivity to pH or ATP were not studied, which limits possible comparisons with the present study.

Sensitivity to pH has been reported for several renal K^+ channels (Wang *et al.* 1997), including the secretory K^+ channel in the CCD apical membrane (and Kir1.1) and the proximal convoluted tubule (PCT) basolateral channel (Wang *et al.* 1990; Mauerer *et al.* 1998*b*; McNicholas *et al.* 1998). The pK_a for the DCT K^+ channel (about 7.6) is more alkaline than that of Kir1.1 (about 7.0–7.2; McNicholas *et al.* 1998). Under standard physiological conditions, the channel activity should lie in the lower part of the dose–response curve, so that slight intracellular alkalinisation would suffice to increase NP_o drastically. Recapitulating the published data for other channel properties, it appears that the DCT basolateral K^+ channel resembles the basolateral PCT channel in terms of conductance, dependence upon the external concentration of K^+ (K_m about 70 mM; Mauerer *et al.* 1998*a*) and sensitivity to internal pH, but differs from it in terms of inward rectification: the DCT channel has a higher affinity towards Mg^{2+} and, unlike the PCT channel, exhibits high sensitivity to spermine. With respect to regulation, two striking differences are that the DCT channel is not inhibited by ATP (Beck *et al.* 1993 ; Mauerer *et al.* 1998*a*) or by high concentrations of Ca^{2+} (Mauerer *et al.* 1998*b*). Inhibition by ATP or Ca^{2+} is also a property of the secretory K^+ channel in the rat CCD (see Wang *et al.* 1997). A final difference is that the activity of the DCT K^+ channel tends to decrease at positive potentials, whereas the K^+

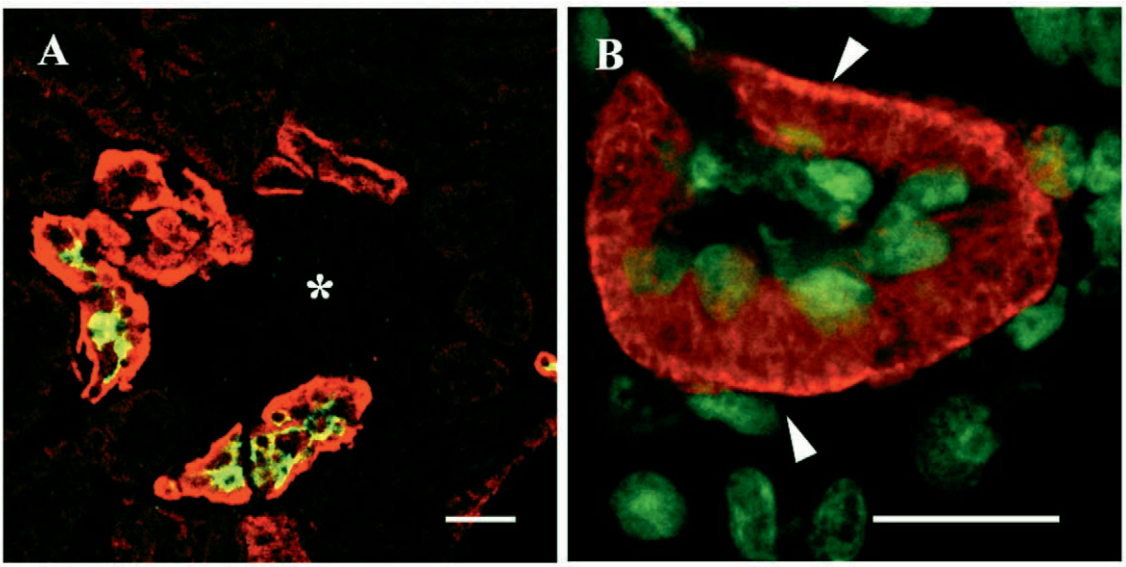

Figure 8. Immunodetection of Kir4.1 in mouse DCT cells

A, frozen mouse kidney sections were double-labelled with anti-Kir4.1 (red) and anti-TSC (green) antibodies and analysed by CLSM. Some, but not all, Kir4.1-positive tubule sections located around the glomerulus (*) were double-labelled with the anti-TSC antibody. Scale bar, 50 μm. *B*, a cortical DCT section labelled with the Kir4.1 antibody (red) and counterstained with Sytox (green) exhibited intense basal membrane staining (arrowheads) associated with an intracellular basal staining. Note that the DCT apical membranes were not stained. Scale bar, 25 μm.

channels in the basolateral membranes of rabbit PCT and CTAL are activated by depolarisation (Parent *et al.* 1988; Hurst *et al.* 1992; Mauerer *et al.* 1998*a*).

Channel rundown after the membrane patch has been detached is a common property of inwardly rectifying K^+ channels. Our results seem to imply that Mg^{2+} is responsible for channel rundown, because the decline in activity was not observed in inside-out patches in the absence of Mg^{2+} or in the presence of 1 mM Ca^{2+}. This contrasts with the PCT channel, which needs Mg^{2+} and ATP (Mauerer *et al.* 1998*a*), but is in keeping with the Kir1.1 channel, which does not run down in the absence of Mg^{2+} (McNicholas *et al.* 1996). The mechanisms by which Mg^{2+} induces a gradual disappearance of channel activity have not been investigated in the present study. It is generally thought that phosphatidylinositol-4,5-biphosphate (PIP_2) modulates positively the activity of several inward rectifier K^+ channels (Huang *et al.* 1998; Yang *et al.* 2000). Therefore channel rundown could be due to the activation of a lipid phosphatase in the presence of Mg^{2+} (Huang *et al.* 1998).

Comparison with cloned, inwardly rectifying K^+ channels

RT-PCR and immunohistochemistry data have demonstrated that there are a number of Kir channels in the mammalian kidney. These include Kir1.1, Kir2.1 (Derst *et al.* 2001), Kir2.3 (Bond *et al.* 1994; Welling, 1997), Kir2.4 (Topert *et al.* 2000), Kir4.1 (Bond *et al.* 1994; Ito *et al.* 1996), Kir4.2 (Shuck *et al.* 1997; Pearson *et al.* 1999), Kir5.1 (Bond *et al.* 1994; Tanemoto *et al.* 2000; Tucker *et al.* 2000), Kir6.1 (Huber *et al.* 2000) and Kir7.1 (Krapivinsky *et al.* 1998; Ookata *et al.* 2000). We can eliminate some of these cloned channels as possible candidates for the DCT K^+ channel on the basis of the functional properties presented here. The Kir1.1 and Kir6.1 channels can be excluded as their hallmark properties, weak inward rectification, insensitivity to spermine (Fakler *et al.* 1994; Yamada & Kurachi, 1995) and, in the case of the Kir6.1 channel, inhibition by ATP (Nichols & Lopatin, 1997) do not match those of the DCT channel. The splice variant, Kir1.1b, is also inhibited by ATP (McNicholas *et al.* 1996, 1998; Wang *et al.* 1997). Some other Kir channels, Kir2.1, Kir2.3 (Welling, 1997), Kir2.4 (Nichols & Lopatin, 1997; Krapivinsky *et al.* 1998), Kir7.1 (Krapivinsky *et al.* 1998) and TWIK1, a channel of the tandem pore family that behaves as an inward rectifier (Lesage & Lazdunski, 2000), also have properties that are in sharp contrast to those of the DCT K^+ channel described here.

When the Kir4.1 channel is expressed alone in a heterologous system, it has a conductance of about 20 pS and displays high P_o (Pessia *et al.* 1996; Tada *et al.* 1998; Yang & Jiang, 1999; Tanemoto *et al.* 2000). It is insensitive to pH in the physiological range (Tanemoto *et al.* 2000; Tucker *et al.* 2000). A pK_a of 6.0 was estimated (Yang & Jiang, 1999; Xu *et al.* 2000; Pessia *et al.* 2001). The inward rectification is usually described as strong (although the g_{in}/g_{out} ratio inferred from Ishii *et al.* (1997) is about 4). The affinity for Mg^{2+} has not been estimated. These properties do not correspond to those of the DCT channel, which has a conductance of about 40 pS, displays a moderate P_o (~0.3) in cell-attached patches, is inhibited by spermine at about 10^{-7} M and is sensitive to pH (pK_a = 7.6). Although Kir4.2 is sensitive to pH (Pearson *et al.* 1999) and shows a pK_a of about 7.1 (Pessia *et al.* 2001), its unitary conductance (Pessia *et al.* 2001) and high P_o (> 0.9) hardly appear to be compatible with those of the DCT K^+ channel.

In contrast, when Kir4.1 is expressed together with Kir5.1 or as a Kir4.1–Kir5.1 concatamer, it has higher unitary conductance (about 30–60 pS) and lower P_o (Pessia *et al.* 1996; Tanemoto *et al.* 2000; Yang *et al.* 2000). Pessia *et al.* (1996) and Yang *et al.* (2000) also report smaller conductance levels, which were only sparsely detected in the case of the DCT K^+ channel. Although whole-cell currents carried by Kir4.1–Kir5.1 channels show strong inward rectification, it has been possible to record outwardly directed unitary currents (Yang *et al.* 2000; Tanemoto *et al.* 2000). The single-channel *i–V* relationship of Kir4.1– Kir5.1 has a g_{in}/g_{out} ratio of about 4 (Yang *et al.* 2000), similar to that observed for the DCT K^+ channel. Most importantly, Kir4.1–Kir5.1 is sensitive to intracellular pH within the physiological range (Xu *et al.* 2000; Tanemoto *et al.* 2000; Tucker *et al.* 2000; Yang *et al.* 2000). Tucker *et al.* (2000) recorded whole oocyte currents while changing the intracellular pH with acetate buffer and obtained a pK_a of 6.9. A more alkaline value was obtained when macroscopic currents in giant inside-out patches (pK_a = 7.45) (Xu *et al.* 2000; Yang *et al.* 2000) or channel currents in conventional inside-out patches (pK_a = 7.35–7.48) (Pessia *et al.* 2001; Yang *et al.* 2000) were recorded. Very recently, it has been shown that Kir4.2–Kir5.1 concatamers have properties that are quite similar to those of Kir4.1–Kir5.1 heteromeric channels: the unitary conductance is about 50 pS, and the channel has a lower P_o than Kir4.2 alone (0.3 *versus* 0.9) and is highly sensitive to pH (pK_a = 7.64) (Pessia *et al.* 2001). Therefore, in the light of present knowledge of these channels, the DCT K^+ channel closely resembles the Kir4.1–Kir5.1 and Kir4.2–Kir5.1 heteromeric channels.

Expression of Kir4.1, Kir4.2 and Kir5.1 channels in the DCT

Ito *et al.* (1996), using immunohistochemical techniques, demonstrated that the Kir4.1 channel was located in the basolateral membranes of the rat distal nephron (DCT and CCD). The present results extend these findings to the mouse species. Indeed, we found that Kir4.1 channels co-localised with TSC, a protein specific to DCT cells, and were located on the basolateral side of mouse DCT cells. Although Kir4.2 (as Kir1.3) is present in the kidney (Shuck

et al. 1997), its exact location along the nephron has not yet been elucidated. Our RT-PCR results suggest that the Kir4.2 channel is present in the mouse DCT, as well as Kir4.1.

Using immunohistochemistry, Tucker *et al.* (2000) have demonstrated the presence of Kir5.1 in both the proximal tubule and the DCT of rat kidney, a finding confirmed by Derst *et al.* (2001) for the proximal tubule using RT-PCR on microdissected renal segments. Tanemoto *et al.* (2000) detected Kir5.1 in rat kidney using Western blot analysis and, most interestingly, showed that Kir4.1 and Kir5.1 co-immunoprecipitate from rat kidney extracts, but not from brain. This is a strong indication that Kir4.1 and Kir5.1 subunits can form heteromeric channels in the kidney. No similar experiments have been attempted on Kir4.2. Since the Kir5.1 antibody designed by Tanemoto *et al.* (2000) is not suitable for immunohistochemistry, we confirmed the presence of Kir5.1 in the mouse DCT using RT-PCR on microdissected tubules. Taken together, the published data and our findings suggest that the Kir4.1, Kir4.2 and Kir5.1 channels are all present in the mouse DCT.

In conclusion, the set of properties displayed by the DCT K^+ channel is not compatible with Kir1.1, Kir2, Kir6.1 channels, or Kir4.1 and Kir4.2 homomeric channels. In contrast, the DCT K^+ channel resembles the Kir4.1–Kir5.1 and the Kir4.2–Kir5.1 heteromeric channels. Since all three subunits are present in the mouse DCT, one or both of these subunit combinations probably underly the K^+ channel described in this study.

REFERENCES

Barry, P. H. & Lynch, J. W. (1991). Liquid junction potentials and small cell effects in patch-clamp analysis. *Journal of Membrane Biology* **121**, 101–117.

Beck, J. S., Hurst, A. M., Lapointe, J. Y. & Laprade, R. (1993). Regulation of basolateral K channels in proximal tubule studied during continuous microperfusion. *American Journal of Physiology* **264**, F496–501.

Bond, C. T., Pessia, M., Xia, X. M., Lagrutta, A., Kavanaugh, M. P. & Adelman, J. P. (1994). Cloning and expression of a family of inward rectifier potassium channels (published erratum appears in *Receptors and Channels* 1994; **2**: following p. 350). *Receptors and Channels* **2**, 183–191.

Chraïbi, A., Van Den Abbeele, T., Guinamard, R. & Teulon, J. (1994). A ubiquitous non-selective cation channel in the mouse renal tubule with variable sensitivity to calcium. *Pflügers Archiv* **429**, 90–97.

Derst, C., Karschin, C., Wischmeyer, E., Hirsch, J. R., Preisig-Muller, R., Rajan, S., Engel, H., Grzeschik, K., Daut, J. & Karschin, A. (2001). Genetic and functional linkage of Kir5.1 and Kir2.1 channel subunits. *FEBS Letters* **491**, 305–311.

Fakler, B., Brandle, U., Bond, C., Glowatzki, E., Konig, C., Adelman, J. P., Zenner, H. P. & Ruppersberg, J. P. (1994). A structural determinant of differential sensitivity of cloned inward rectifier K^+ channels to intracellular spermine. *FEBS Letters* **356**, 199–203.

Glowatzki, E., Fakler, G., Brandle, U., Rexhausen, U., Zenner, H. P., Ruppersberg, J. P. & Fakler, B. (1995). Subunit-dependent assembly of inward-rectifier K^+ channels. *Proceedings of the Royal Society* B **261**, 251–261.

Hamill, O. P., Marty, A., Neher, E., Sakmann, B. & Sigworth, F. J. (1981). Improved patch-clamp techniques for high-resolution current recording from cells and cell-free membrane patches. *Pflügers Archiv* **391**, 85–100.

Huang, C.-L., Feng, S. & Hilgemann, D. W. (1998). Direct activation of inward rectifier potassium channels by PIP_2 and its stabilisation by $G_{\beta\gamma}$. *Nature* **391**, 803–806.

Huber, S. M., Braun, G. S., Segerer, S., Veh, R. W. & Horster, M. F. (2000). Metanephrogenic mesenchyme-to-epithelium transition induces profound expression changes of ion channels. *American Journal of Physiology – Renal Physiology* **279**, F65–76.

Hummler, E., Barker, P., Gatzy, J., Beermann, F., Verdumo, C., Schmidt, A., Boucher, R. & Rossier, B. C. (1996). Early death due to defective neonatal lung liquid clearance in α-ENaC-deficient mice. *Nature Genetics* **12**, 325–328.

Hunter, M. (1991). Potassium-selective channels in the basolateral membrane of single proximal tubule cells of frog kidney. *Pflügers Archiv* **418**, 26–34.

Hurst, A. M., Duplain, M. & Lapointe, J. Y. (1992). Basolateral membrane potassium channels in rabbit cortical thick ascending limb. *American Journal of Physiology* **263**, F262–267.

Ishii, M., Horio, Y., Tada, Y., Hibino, H., Inanobe, A., Ito, M., Yamada, M., Gotow, T., Uchiyama, Y. & Kurachi, Y. (1997). Expression and clustered distribution of an inwardly rectifying potassium channel, KAB-2/Kir4.1, on mammalian retinal Muller cell membrane: their regulation by insulin and laminin signals. *Journal of Neuroscience* **17**, 7725–7735.

Ito, M., Inanobe, A., Horio, Y., Hibino, H., Isomoto, S., Ito, H., Mori, K., Tonosaki, A., Tomoike, H. & Kurachi, Y. (1996). Immunolocalization of an inwardly rectifying K^+ channel, K(AB)-2 (Kir4.1), in the basolateral membrane of renal distal tubular epithelia. *FEBS Letters* **388**, 11–15.

Krapivinsky, G., Medina, I., Eng, L., Krapivinsky, L., Yang, Y. & Clapham, D. E. (1998). A novel inward rectifier K^+ channel with unique pore properties. *Neuron* **20**, 995–1005.

Lesage, F. & Lazdunski, M. (2000). Potassium channels with two pore domains. In *Pharmacology of Ionic Channel Function. Activators and Inhibitors*, vol. 147, ed. Endo, M., Kurachi, Y. & Mishina, M., pp. 333–346. Springer, Berlin.

McNicholas, C. M., MacGregor, G. G., Islas, L. D., Yang, Y., Hebert, S. C. & Giebisch, G. (1998). pH-dependent modulation of the cloned renal K^+ channel, ROMK. *American Journal of Physiology* **275**, F972–981.

McNicholas, C. M., Yang, Y., Giebisch, G. & Hebert, S. C. (1996). Molecular site for nucleotide binding on an ATP-sensitive renal K^+ channel (ROMK2). *American Journal of Physiology* **271**, F275–285.

Matsuda, H. (1991*a*). Effects of external and internal K^+ ions on magnesium block of inwardly rectifying K^+ channels in guinea-pig heart cells. *Journal of Physiology* **435**, 83–99.

Matsuda, H. (1991*b*). Magnesium gating of the inwardly rectifying K^+ channel. *Annual Review of Physiology* **53**, 289–298.

Mauerer, U. R., Boulpaep, E. L. & Segal, A. S. (1998*a*). Properties of an inwardly rectifying ATP-sensitive K^+ channel in the basolateral membrane of renal proximal tubule. *Journal of General Physiology* **111**, 139–160.

Maurer, U. R., Boulpaep, E. L. & Segal, A. S. (1998*b*). Regulation of an inwardly rectifying ATP-sensitive K^+ channel in the basolateral membrane of renal proximal tubule. *Journal of General Physiology* **111**, 161–180.

Nichols, C. G., Ho, K. & Hebert, S. (1994). Mg^{2+}-dependent inward rectification of ROMK1 potassium channels expressed in *Xenopus* oocytes. *Journal of Physiology* **476**, 399–409.

Nichols, C. G. & Lopatin, A. N. (1997). Inward rectifier potassium channels. *Annual Review of Physiology* **59**, 171–191.

Ookata, K., Tojo, A., Suzuki, Y., Nakamura, N., Kimura, K., Wilcox, C. S. & Hirose, S. (2000). Localization of inward rectifier potassium channel kir7.1 in the basolateral membrane of distal nephron and collecting duct. *Journal of the American Society of Nephrology* **11**, 1987–1994.

Parent, L., Cardinal, J. & Sauve, R. (1988). Single-channel analysis of a K channel at basolateral membrane of rabbit proximal convoluted tubule. *American Journal of Physiology* **254**, F105–113.

Pearson, W. L., Dourado, M., Schreiber, M., Salkoff, L. & Nichols, C. G. (1999). Expression of a functional Kir4 family inward rectifier K^+ channel from a gene cloned from mouse liver. *Journal of Physiology* **514**, 639–653.

Pessia, M., Imbrici, P., D'Adamo, M. C., Salvatore, L. & Tucker, S. J. (2001). Differential pH sensitivity of Kir4.1 and Kir4.2 potassium channels and their modulation by heteropolymerisation with Kir5.1. *Journal of Physiology* **532**, 359–367.

Pessia, M., Tucker, S. J., Lee, K., Bond, C. T. & Adelman, J. P. (1996). Subunit positional effects revealed by novel heteromeric inwardly rectifying K^+ channels. *EMBO Journal* **15**, 2980–2987.

Plotkin, M. D., Kaplan, M. R., Verlander, J. W., Lee, W. S., Brown, D., Poch, E., Gullans, S. R. & Hebert, S. C. (1996). Localization of the thiazide sensitive Na-Cl cotransporter, rTSC1 in the rat kidney. *Kidney International* **50**, 174–183.

Reilly, R. F. & Ellison, D. H. (2000). Mammalian distal tubule: physiology, pathophysiology, and molecular anatomy. *Physiological Reviews* **810**, 277–313.

Shuck, M. E., Piser, T. M., Bock, J. H., Slightom, J. L., Lee, K. S. & Bienkowski, M. J. (1997). Cloning and characterization of two K^+ inward rectifier (Kir) 1.1 potassium channel homologs from human kidney (Kir1.2 and Kir1.3). *Journal of Biological Chemistry* **272**, 586–593.

Tada, Y., Horio, Y. & Kurachi, Y. (1998). Inwardly rectifying K^+ channel in retinal Muller cells: comparison with the KAB-2/Kir4.1 channel expressed in HEK293T cells. *Japanese Journal of Physiology* **48**, 71–80.

Taglialatela, M., Ficker, E., Wible, B. A. & Brown, A. M. (1995). C-terminus determinants for Mg^{2+} and polyamine block of the inward rectifier K^+ channel IRK1. *EMBO Journal* **14**, 5532–5541.

Tanemoto, M., Kittaka, N., Inanobe, A. & Kurachi, Y. (2000). *In vivo* formation of a proton-sensitive K^+ channel by heteromeric subunit assembly of Kir5.1 with Kir4.1. *Journal of Physiology* **525**, 587–592.

Taniguchi, J., Yoshitomi, K. & Imai, M. (1989). K^+ channel currents in basolateral membrane of distal convoluted tubule of rabbit kidney. *American Journal of Physiology* **256**, F246–254.

Teulon, J., Paulais, M. & Bouthier, M. (1987). A Ca^{2+}-activated cation-selective channel in the basolateral membrane of the cortical thick ascending limb of Henle's loop of the mouse. *Biochimica et Biophysica Acta* **905**, 125–132.

Topert, C., Doring, F., Derst, C., Daut, J., Grzeschik, K. H. & Karschin, A. (2000). Cloning, structure and assignment to chromosome 19q13 of the human Kir2.4 inwardly rectifying potassium channel gene (KCNJ14). *Mammalian Genome* **11**, 247–249.

Tucker, S. J., Imbrici, P., Salvatore, L., D'Adamo, M. C. & Pessia, M. (2000). pH dependence of the inwardly rectifying potassium channel, Kir5.1, and localization in renal tubular epithelia. *Journal of Biological Chemistry* **275**, 16404–16407.

Vandewalle, A., Cluzeaud, F., Bens, M., Kieferle, S., Steinmeyer, K. & Jentsch, T. J. (1997). Localization and induction by dehydration of ClC-K chloride channels in the rat kidney. *American Journal of Physiology* **272**, F678–688.

Wang, W., Hebert, S. C. & Giebisch, G. (1997). Renal K^+ channels: structure and function. *Annual Review of Physiology* **59**, 413–436.

Wang, W., Schwab, A. & Giebisch, G. (1990). Regulation of small-conductance K^+ channel in apical membrane of rat cortical collecting tubule. *American Journal of Physiology* **259**, F494–502.

Welling, P. A. (1997). Primary structure and functional expression of a cortical collecting duct Kir channel. *American Journal of Physiology* **273**, F825–836.

Wible, B. A., Taglialatela, M., Ficker, E. & Brown, A. M. (1994). Gating of inwardly rectifying K^+ channels localized to a single negatively charged residue. *Nature* **371**, 246–249.

Woodhull, A. M. (1973). Ionic blockage of sodium channels in nerve. *Journal of General Physiology* **61**, 687–708.

Xu, H., Cui, N., Yang, Z., Qu, Z. & Jiang, C. (2000). Modulation of Kir4.1 and Kir5.1 by hypercapnia and intracellular acidosis. *Journal of Physiology* **524**, 725–735.

Yamada, M. & Kurachi, Y. (1995). Spermine gates inward-rectifying muscarinic but not ATP-sensitive K^+ channels in rabbit atrial myocytes. Intracellular substance-mediated mechanism of inward rectification. *Journal of Biological Chemistry* **270**, 9289–9294.

Yamashita, T., Horio, Y., Yamada, M., Takahashi, N., Kondo, C. & Kurachi, Y. (1996). Competition between Mg^{2+} and spermine for a cloned IRK2 channel expressed in a human cell line. *Journal of Physiology* **493**, 143–156.

Yang, Z. & Jiang, C. (1999). Opposite effects of pH on open-state probability and single channel conductance of Kir4.1 channels. *Journal of Physiology* **520**, 921–927.

Yang, Z., Xu, H., Cui, N., Qu, Z., Chanchevalap, S., Shen, W. & Jiang, C. (2000). Biophysical and molecular mechanisms underlying the modulation of heteromeric Kir4.1-Kir5.1 channels by CO2 and pH. *Journal of General Physiology* **116**, 33–45.

Yoshitomi, K., Shimizu, T., Taniguchi, J. & Imai, M. (1989). Electrophysiological characterization of rabbit distal convoluted tubule cell. *Pflügers Archiv* **414**, 457–463.

Acknowledgements

We wish to thank Dr S. C. Hebert (Vanderbilt University, Nashville, Tennesse, USA) for providing us with valuable antibodies. This study was funded by INSERM and Contrat Prisme INSERM (J.T. and M.P.). S. Lourdel holds a fellowship from the Ministère de la Recherche and J. Teulon is a CNRS researcher. The English text was checked by Monika Ghosh.